Molecular photodissociation with diverging couplings: An application to H_2^+ in intense cw laser fields. I. The single-photon problem

M. Chrysos, O. Atabek, and R. Lefebvre*
Laboratoire de Photophysique Moléculaire, Centre National de la Recherche Scientifique, Bâtiment 213, Campus d'Orsay, 91405 Orsay CEDEX, France
(Received 18 February 1993; revised manuscript received 22 June 1993)

The photodissociation of homonuclear ions exposed to continuous-wave (cw) lasers gives rise to asymptotically diverging couplings when approached in the electric-field gauge. Quantization of the laser-induced resonances becomes possible by complex rotation, leading to accurate energies, widths, and wave functions. A pseudoflux is endowed in the closed-channel component when calculated in the diabatic frame and for high laser intensities. A complex energy flux analysis performed in the adiabatic representation is developed, replacing the standard Siegert analysis which is no longer adequate for the extraction of the width from the asymptotic amplitude of the open-channel function. At the limit of strong radiative couplings the remaining nonadiabatic couplings asymptotically vanish. In the special case of constant potential couplings, the width is given by the asymptotic amplitude of the open-channel function through a modified Siegert analysis. Application is made to H_2^+, in laser frequency and intensity regimes where a single-photon description is sufficient.

PACS number(s): 33.80.Gj, 42.50.Hz, 34.50.Rk, 34.10.+x

I. INTRODUCTION

The quantitative study of photofragmentation dynamics under strong radiation fields constitutes one of the challenging problems of molecular physics. Optical nonlinearities and important distorsions of absorption line shapes have been experimentally observed in dissociation processes involving even a single photon [1]. A considerable amount of theoretical effort has recently been devoted to the description and interpretation of the inherent mechanisms leading to the aforementioned effects [2–8]. The field can no longer be considered as a perturbation, and an exact treatment has to take properly into account the molecule-plus-laser field system as a whole. Conceptually, this can be viewed in two different ways. The first is within a time-dependent approach [9–11]. It offers the possibility to study the realistic time-resolved dynamics of the process basically driven by an intense electromagnetic field, which in general can only be achieved using short laser pulses. The spreading of the wave packet or the possible presence of long-lived resonances which govern the process may, however, lead to hard computational tasks when this approach is addressed. For pulses of long duration with respect to the time scale of the dynamics of the process, the laser field can be considered as periodic, thus allowing the complete elimination of the time variable through a full Floquet expansion of the molecule-plus-field Hamiltonian. This gives rise to the time-independent approach. This approach not only provides a more direct and accurate way to calculate the resonances involved in the process, but also offers a useful and important interpretative tool in terms of the stationary field dressed molecular states [5,8,12–14].

Within a time-independent approach, essential complications arise when referring to a continuous-wave (cw) laser acting on homonuclear molecular ions. As is well known, the radiative coupling within the dipole approximation may be introduced through two different gauges: the radiative field (RF) gauge $\vec{A}\cdot\vec{p}$ (i.e., the vector potential $\vec{A}$ times the momentum vector $\vec{p}$), or the electric-field (EF) gauge $\vec{\mu}\cdot\vec{E}$ (i.e., the transition dipole moment $\vec{\mu}$ times the electric-field vector $\vec{E}$). Both are equivalent, but present different pros and cons [15,16]. With respect to the RF gauge, interchannel couplings dramatically increase at short internuclear distances, thus requiring the introduction of a considerable amount of excited electronic states for an appropriate description. This is basically why the present analysis is going to be held to the EF gauge, which nevertheless presents another difficulty related to a spatially diverging dipole transition moment. In the case of H_2^+, the unique electron of the system is equally shared between the two protons, leading at the separated-atom limit to a configuration H^+-electron-H^+. The dipole moment consequently acquires asymptotically a diverging $R/2$ spatial dependence [17], giving rise to so-called *persistent* effects. Such effects appear in various contexts in atomic and molecular physics: Stark effect, spin-orbit couplings, Coriolis or hyperfine interactions [18–21]. They result from potential matrices which either do not go to constant thresholds (persistent potentials) or do not converge to diagonal forms at the separated fragment limit (persistent couplings). In the case of the single-photon absorption of H_2^+ described by a single Floquet block which involves one open and one closed channel, a standard scattering theoretical approach in the diabatic representation is no longer appropriate to describe experimental observations. This is due to the fact that the fragments remain coupled at an infinite interparticle distance through a potential matrix having asymptotically diverging off-diagonal elements (persistent couplings). When moving to the adiabatic representation, the interchannel coupling is diagonalized, but the per-

sistent effects are transferred into both nonadiabatic couplings and adiabatic potentials which behave as $\pm R/2$ at infinite interparticle distances (persistent potentials). Moreover, a Siegert-type characterization for the resonances [i.e., a regular solution of the Schrödinger equation with outgoing $\exp(ikR)$ behavior in each open fragmentation channel] [22] is impossible: in the diabatic frame this is due to asymptotically nonvanishing interchannel radiative couplings, and in the adiabatic frame to asymptotically nonconstant potentials.

The complex-coordinate method has recently been presented as a possible way to circumvent such difficulties [8,21,23]. In particular, it has been shown that by rotating the integration coordinate R into the complex plane, even in cases where interchannel couplings and/or channel potentials asymptotically diverge, resonances can still be defined as solutions of an eigenvalue problem with zero boundary conditions at the origin and at large interparticle separation [18,21]. These conditions give rise to complex quantized energies providing the positions and the total widths of the laser induced resonances. In the case of H_2^+, they have been calculated for several wavelength and intensity regimes. The aim of this paper is to develop an alternative way to evaluate the same [8,23] rates, but referring now to the open-channel component of the resonance wave function in the adiabatic representation. The advantage of such a method is to provide additional physical insight into the dynamics of the process within an original R-dependent flux analysis which is to be developed (this paper), and the possibility, through a following multichannel generalization (paper II) [24], to calculate partial fluxes and branching ratios of multiphoton processes resulting into different fragment states.

Besides this quantal approach, we note that semiclassical treatments extensively developed in the literature [25] also seem adequate for handling persistent effects, as they rely upon adiabatic potentials. Nevertheless, their use presents some difficulties related to an accurate determination of phase correction factors which has to go beyond an approximation of the Landau-Zener type. This approximation is clearly no longer valid in the presence of persistent couplings, due to the fact that it assumes that potential couplings are localized at the curve-crossing position. As for the application of a multichannel semiclassical approach, it becomes even harder since it goes beyond standard curve-crossing situations.

II. THEORY

A. The width from energy quantization

The calculation of resonance energies and wave functions can in principle be done with either a real or a complex variable [26]. The latter choice turns out to be a powerful tool for the accurate and easy localization of the resonances even in cases deviating from the standard scattering matrix analysis [27]. The coordinate R is rotated into the complex plane as [28,29]

$$R \rightarrow \begin{cases} \rho = R & \text{for } R \le R_0 \\ \rho = R_0 + (R - R_0)\exp(i\theta) & \text{for } R \ge R_0 \ . \end{cases} \tag{1}$$

The parameter R_0 allows for a partially real integration path to be constructed, which, in some cases, turns out to be of decisive importance for the accurate localization of the resonance wave functions. In a converged calculation the resonance properties must remain, to some extent, insensitive to changes of these parameters, thus forming well-defined plateaus of stability.

The two-channel close-coupled equations are solved in the diabatic representation. They read [5,8]

$$\left[-\frac{d^2}{d\rho^2} + \frac{J(J+1)}{\rho^2} + V_d(\rho) - E \right] U_1(\rho) + V_{\text{int}}(\rho) U_2(\rho) = 0 \ , \tag{2}$$

$$\left[-\frac{d^2}{d\rho^2} + \frac{J(J+1)}{\rho^2} + V_g(\rho) + \hbar\omega - E \right] U_2(\rho) + V_{\text{int}}(\rho) U_1(\rho) = 0 \ , \tag{3}$$

where J denotes the rotation quantum number, while the mass factor has been embodied in a properly scaled coordinate ρ [30]. The quantities V_g and V_d denote the diabatic potentials corresponding to the ground $1s\sigma_g\ ^1\Sigma_g^+$ and excited $2p\sigma_u\ ^1\Sigma_u^+$ electronic states, respectively, of H_2^+ given by Bunkin and Tugov [31]. U_1 and U_2 are the open- and closed-channel components of the diabatic nuclear wave function. The interchannel coupling $V_{\text{int}}(R)$ is given by [17]

$$V_{\text{int}}(\rho) = 1.17 \times 10^{-3} \sqrt{I}\, \mu(\rho) \ , \tag{4}$$

where μ is in atomic units, and I the laser intensity in W/cm^2, leading to V_{int} in cm^{-1}. The functional form of μ corresponds to an asymptotically divergent transition dipole [31]. In order to solve this system, the Fox-Goodwin propagation algorithm is used in conjunction with a properly chosen set of imposed boundary conditions which accounts for the correct behavior of the channel wave functions at short and large distances. The algorithm consists in an iterating sequence of two steps [30].

(i) Properly initialized 2×2 Fox-Goodwin matrices $\mathbf{P}^i$ and $\mathbf{P}^o$ are constructed at each point m of a grid, in terms of independent solution matrices $\mathbf{U}^i$ and $\mathbf{U}^o$:

$$\mathbf{P}_m^i = \mathbf{U}_{m+1}^i [\mathbf{U}_m^i]^{-1}, \quad \mathbf{P}_m^o = \mathbf{U}_{m-1}^o [\mathbf{U}_m^o]^{-1} \ , \tag{5}$$

and propagated along the grid inward (label i) and outward (label o), respectively.

(ii) The criterion for convergence is a determinantal condition which must be obeyed by the matrices at a matching point chosen at will:

$$\det | \mathbf{P}_M^i - [\mathbf{P}_{M+1}^o]^{-1} | = 0 \ , \tag{6}$$

where index M labels the matching position on the grid. For regular open-channel components with purely outgoing asymptotic behavior, this condition is fulfilled only for complex resonance energies E. Their real part E_r corresponds to the position of the resonance, while their imaginary part gives rise to the resonance width Γ.

As regards the problem of the boundary conditions to

be imposed, it addresses the initialization of the Fox-Goodwin matrices $\mathbf{P}^i$ and $\mathbf{P}^o$. Given that near the origin both open and closed channels are classically forbidden, regularity can be imposed for both channel functions:

$$U_1(\rho=0)=U_2(\rho=0)=0 \ . \tag{7}$$

Therefore, the Fox-Goodwin matrix $\mathbf{P}^o$ can be safely initialized by zero for both the open and closed channels. As for the boundary conditions for large interparticle distances, for standard situations, characterized by channel potentials tending to constant thresholds and by asymptotically vanishing couplings, the potential matrix acquires a constant diagonal form. The open-channel component of the resonance wave function takes the well-known Siegert form [22]:

$$U_1(R)\rightarrow A\exp(ikR) \quad \text{as } R\rightarrow\infty \ , \tag{8}$$

where $k=\sqrt{E}$ is the wave number in the open channel, and A is the corresponding amplitude. Also, in cases characterized by persistent effects, the asymptotic form of the open-channel function is different from the standard Siegert, and depends on the form of the involved potentials and couplings. It can, however, be shown [18] that complex rotation of the coordinate may, even in such situations, produce localized channel functions:

$$U_1(\rho\rightarrow\infty)=U_2(\rho\rightarrow\infty)=0 \ . \tag{9}$$

As for the corresponding ratio matrix, recently Chrysos and Lefebvre demonstrated that if complex rotation is used then $\mathbf{P}^i$ initialized by zero for all the channels is able to correctly build resonance wave functions even in cases where the interchannel couplings persist at infinity [21]. The resonance solutions are as accurate as those obtained by a real coordinate treatment, in which the correct outgoing asymptotic behavior of the open-channel components has to be taken into account.

B. The width from the wave function

An appropriate asymptotic analysis of the resonance wave function can also lead to accurate determination of the width. The prerequisite for such an analysis is the calculation of channel components $U_1(\rho)$ and $U_2(\rho)$. At the matching position M the channel functions can be obtained by solving the homogeneous set of equations

$$[\mathbf{P}^i_M-(\mathbf{P}^o_{M+1})^{-1}]\underline{U}_M=0 \ , \tag{10}$$

where $\underline{U}_M$ denotes the solution column vector with components U_j at M. The channel functions at the other grid points could in principle be constructed by making use of the relations [32]

$$\underline{U}_{M+1}=(\mathbf{P}^o_{M+1})\underline{U}_M, \quad \underline{U}_{M-1}=(\mathbf{P}^i_{M-1})^{-1}\underline{U}_M \ . \tag{11}$$

However, when leaving the matching point, divergence of the wave function is very likely toward classically forbidden regions where its components must tend to zero (i.e., toward small R for all channels or toward large R for closed channels). A much more satisfactory computational procedure can be invoked that is based on the following fact: once the iterative method giving the resonance energy has converged, throughout the entire grid we have

$$(\mathbf{P}^o_{m+1})^{-1}=\mathbf{P}^i_m, \quad (\mathbf{P}^i_{m-1})^{-1}=\mathbf{P}^o_m \ . \tag{12}$$

Provided that all these matrices have been stored, $\mathbf{P}^i$ can be used to perform *outward* propagation of the vector solution, while $\mathbf{P}^o$ is used for *inward* propagation. This procedure omits completely the instabilities which are observed when $\mathbf{P}^o$ and $\mathbf{P}^i$ are used to perform outward and inward propagations, respectively. The high reliability of this technique has been recently demonstrated [33].

The computed channel functions $U_1(\rho)$ and $U_2(\rho)$ are arbitrarily normalized. The correct normalization of the wave function, however, remains a difficult task, and a large part of the currently existing treatments of resonances has been devoted to this problem ([34,35] and references therein). Various methods of normalization of open-channel functions exist. At least two of them deserve special attention.

Normalization 1

The integration of the squares of the rotated channel functions is carried out along a partially real path C defined by Eq. (1) [34]:

$$\begin{aligned}\int_C[U_1^2(\rho)+U_2^2(\rho)]d\rho &= \int_0^{R_0}[U_1^2(R)+U_2^2(R)]dR \\ &\quad +\exp(i\theta)\int_{R_0}^{\infty}[U_1^2(\rho)+U_2^2(\rho)]dR \ .\end{aligned} \tag{13}$$

The integrand is square integrable and the integral converges to a complex number. Both the modulus and phase of the normalization coefficient have been stored in this quantity. Let us further make the assumption that at distance R_0 the closed channels have already died, while the open channels are just starting to acquire Siegert asymptotic behavior. Then Eq. (13) via Eq. (8) takes the form

$$\begin{aligned}\int_C[U_1^2(\rho)+U_2^2(\rho)]d\rho &= \int_0^{R_0}[U_1^2(R)+U_2^2(R)]dR+\frac{i}{2k}U_1^2(R_0) \ .\end{aligned} \tag{14}$$

Although path C is θ dependent, the latter expression turns out to possess a basic property for a normalization constant, namely the θ invariance. Normalized channel functions can be defined as

$$\tilde{U}_1=U_1\Big/\left[\int_0^{R_0}[U_1^2(R)+U_2^2(R)]dR+\frac{i}{2k}U_1^2(R_0)\right]^{1/2} , \tag{15}$$

$$\tilde{U}_2=U_2\Big/\left[\int_0^{R_0}[U_1^2(R)+U_2^2(R)]dR+\frac{i}{2k}U_1^2(R_0)\right]^{1/2} . \tag{16}$$

Normalized amplitudes for the channel functions can also be defined. For the open-channel component it reads

$$\tilde{A}=A\Big/\left[\int_0^{R_0}[U_1^2(R)+U_2^2(R)]dR+\frac{i}{2k}U_1^2(R_0)\right]^{1/2}. \tag{17}$$

According to the theory of Fano [36], the total width of the resonance can be written as

$$\frac{\Gamma}{2}=|k||\tilde{A}|^2 . \tag{18}$$

Equations (14) and (18) are identical to those produced by Hokkyo [37,35] and obtained from S-matrix considerations.

Normalization 2

This refers to the square of the modulus of each channel function, integrated up to a certain distance R [38]. No complex rotation is assumed for this normalization, and the quantity R_0 ($<R$) is retained only to indicate a certain position in the far asymptotic region. By making the same assumptions as for normalization 1 with respect to the asymptotic behavior of the channel functions, it can be shown that the following diverging expression is obtained:

$$\int_0^R[|U_1(R')|^2+|U_2(R')|^2]dR' = \int_0^{R_0}[|U_1(R')|^2+|U_2(R')|^2]dR' + \frac{1}{2k_1}(|U_1(R)|^2-|U_1(R_0)|^2) , \tag{19}$$

where $-k_1$ (<0) denotes the imaginary part of the wave number k (its real part being $k_0>0$). This behavior is inappropriate for a normalization coefficient. The indispensable R invariance emerges by extracting the diverging asymptotic behavior of Eq. (19), thus giving rise to normalized channel functions [21,38]:

$$\tilde{U}_1=U_1\Big/\left[\int_0^{R_0}[|U_1(R')|^2+|U_2(R')|^2]dR' + \frac{|A|^2}{2k_1}(1-e^{2k_1R_0})\right]^{1/2}, \tag{20}$$

$$\tilde{U}_2=U_2\Big/\left[\int_0^{R_0}[|U_1(R')|^2+|U_2(R')|^2]dR' + \frac{|A|^2}{2k_1}(1-e^{2k_1R_0})\right]^{1/2}. \tag{21}$$

The normalized amplitude for the open-channel component of the resonance wave function reads

$$\tilde{A}=A\Big/\left[\int_0^{R_0}[|U_1(R')|^2+|U_2(R')|^2]dR' + \frac{|A|^2}{2k_1}(1-e^{2k_1R_0})\right]^{1/2}. \tag{22}$$

The latter expression has been discussed by Humblet and Rosenfeld [38], and leads to a total width

$$\frac{\Gamma}{2}=k_0|\tilde{A}|^2 . \tag{23}$$

For narrow resonances and in the absence of any persistent effects, Eqs. (18) and (23) are expected to be very close to each other, reproducing to a very good approximation the width which is extracted from energy quantization. For H_2^+ in a weak-intensity regime, this is exactly the case. The approximation of asymptotically decoupled channels converging to constant thresholds is still reasonable. As the intensity increases, the asymptotic form of the open channel departs more and more from the conventional Siegert form. For such intensities, both Eqs. (18) and (23) are expected to fail.

A more general way of extracting the resonance properties, valid even for high intensities, is found in the context of a complex-energy probability-flux analysis and does not assume any particular asymptotic behavior for the open-channel component of the resonance wave function. To this purpose, let us multiply Eqs. (2) and (3) by U_1^* and U_2^*, respectively, and add them up. By subtracting from the resulting expression its complex conjugate, one gets

$$(E-E^*)[|U_1|^2+|U_2|^2]+[U_1^*U_1''-U_1U_1''^*]+[U_2^*U_2''-U_2U_2''^*]=0 . \tag{24}$$

Given that $\Gamma=-\mathrm{Im}(E-E^*)$, Eq. (24) leads directly to the following expression:

$$\frac{\Gamma}{2}=\mathrm{Im}[U_1^*(R)U_1''(R)+U_2^*(R)U_2''(R)]/[|U_1(R)|^2+|U_2(R)|^2],\quad R\le R_0 . \tag{25}$$

By integrating Eq. (25), a *flux* expression is obtained:

$$\frac{\Gamma}{2}=\mathrm{Im}[U_1^*(R)U_1'(R)+U_2^*(R)U_2'(R)]\Big/\int_0^R[|U_1(R')|^2+|U_2(R')|^2]dR',\quad R\le R_0 . \tag{26}$$

So far, the concept of probability flux has been thoroughly examined in both time-dependent [39] and time-independent approaches [40–42], and by treating either real [40,41] or complex [42] energies. Nevertheless, all the situations which have been studied refer to potential matrices converging to constant and diagonal forms (see for instance [41]). Both Eqs. (25) and (26) are R invariant. For their derivation no approximation has been as-

sumed. They are valid whatever the potential channels or the interchannel couplings are. In addition, no specific asymptotic form has been imposed on the behavior of the channel functions. This fact makes them valid throughout the entire real range of R.

For standard situations of potential channels converging to constant thresholds, and interchannel couplings vanishing asymptotically, only the first term of Eq. (25) survives asymptotically. The term which refers to the closed-channel component vanishes at large interparticle distances, and the corresponding flux to the closed channel asymptotically dies out as it has to (see also Fig. 1). At large distances where U_2 is expected to be vanishingly small, the resonance width is merely given by

$$\frac{\Gamma}{2} \simeq \mathrm{Im}\left[\frac{U_1''(R)}{U_1(R)}\right] . \tag{27}$$

Its energy position reads

$$E_r \simeq V_1(R) - \mathrm{Re}\left[\frac{U_1''(R)}{U_1(R)}\right] . \tag{28}$$

In these expressions only the open-channel component is involved [43]. For situations characterized by persistent effects, this approximation is no longer valid. The closed-channel component is strongly driven by the open channel, thus endowing asymptotically a physically unacceptable flux. Another pair of channel functions is sought, such that the information for both width and shift is to be carried by only one of the new channels, the other vanishing asymptotically. The linear combination of U_1 and U_2 which gives rise to channel functions with the desired property will be shown to be the one which eliminates the persistent potential coupling. This combination is determined by diagonalizing the potential matrix $\mathbf{V}(R)$, resulting in adiabatic eigenvalues $V_{\pm}(R)$ which are given by

$$V_{\pm}(R) = \frac{V_1(R)+V_2(R)}{2} \pm \left[\left[\frac{V_1(R)-V_2(R)}{2}\right]^2 + V_{\mathrm{int}}^2(R)\right]^{1/2} . \tag{29}$$

The corresponding adiabatic channel wave functions $U_{\pm}(R)$ are

$$U_+(R) = U_1(R)\cos\phi(R) - U_2(R)\sin\phi(R) , \tag{30}$$

$$U_-(R) = U_1(R)\sin\phi(R) + U_2(R)\cos\phi(R) , \tag{31}$$

where $\phi(R)$ is defined as

$$\tan\phi(R) = \frac{V_{\mathrm{int}}(R)}{V_2(R)-V_+(R)} . \tag{32}$$

By expressing the diabatic functions in Eqs. (30) and (31) as linear combinations of the adiabatic ones, and substituting the resulting expressions in both Eqs. (26) and (25), two new expressions are obtained:

$$\frac{\Gamma}{2} = \frac{\mathrm{Im}[U_+^*(R)U_+'(R) + U_-^*(R)U_-'(R)]}{\int_0^R [|U_+(R')|^2 + |U_-(R')|^2]dR'} + 2\frac{\mathrm{Im}[U_+^*(R)U_-(R)\phi'(R)]}{\int_0^R [|U_+(R')|^2 + |U_-(R')|^2]dR'} \tag{33}$$

and

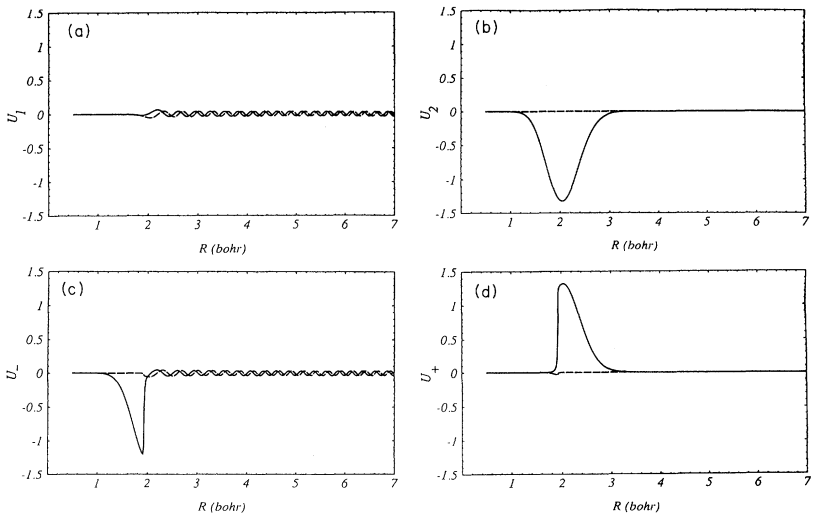

FIG. 1. Real (solid lines) and imaginary (dashed lines) parts of the channel components of the $v=0$ resonance wave function for $I=3.5\times10^{10}$ W/cm^2. The functions are normalized according to Eqs. (15) and (16), which preserve the phase factors. (a) Open channel in the diabatic frame. (b) Closed channel in the diabatic frame. (c) Open channel in the adiabatic frame. (d) Closed channel in the adiabatic frame. Asymptotically the closed-channel components are vanishingly small in both diabatic and adiabatic frames, while their imaginary part is negligible everywhere. The real and imaginary parts of the open-channel components differ asymptotically by a phase approximately equal to $\pi/2$.

$$\frac{\Gamma}{2}=\frac{\mathrm{Im}[U_+^*(R)U_+''(R)+U_-^*(R)U_-''(R)]}{|U_+(R)|^2+|U_-(R)|^2}$$
$$+2\frac{\mathrm{Im}[U_+^{*\prime}U_-\phi'+U_+^*U_-'\phi'+U_+^*U_-\phi'']}{|U_+(R)|^2+|U_-(R)|^2}\ . \quad (34)$$

In these expressions, apart from the two single-channel terms, interference terms appear, related to nonadiabatic couplings which spring out once the potential couplings are eliminated. In order to determine their dependence as a function of increasing intensity, let us examine the quantity $\phi'(R)$ for interparticle distances at which the diabatic potentials have reached their threshold values. By making use of Eq. (32), $\phi'(R)$ becomes

$$\phi'=\frac{V_{\mathrm{int}}'}{f}\frac{\left[f-\frac{\hbar\omega}{2}\right]\frac{\hbar\omega}{2}}{V_{\mathrm{int}}^2+\left[f-\frac{\hbar\omega}{2}\right]^2}\ , \quad (35)$$

where

$$f=\left[\left[\frac{\hbar\omega}{2}\right]^2+V_{\mathrm{int}}^2\right]^{1/2}\ . \quad (36)$$

Two extreme regimes of interchannel coupling V_{int} can be examined in the region where the fragmentation occurs, as compared to the dressing energy $\hbar\omega$:

(i) $|V_{\mathrm{int}}/\hbar\omega|\ll 1$: This is the regime to which the present study refers. Even for the highest examined intensity ($I=1.4\times10^{13}$ W/cm^2), the dressing energy which corresponds to the selected wavelength ($\hbar\omega=10^5$ cm^{-1}) by far dominates over the interchannel coupling throughout the region which is important for the fragmentation to occur (e.g., $|V_{\mathrm{int}}/\hbar\omega|\simeq 0.14$ at $R=7$ bohr). The expression of Eq. (36) can be linearized, and Eq. (35) becomes

$$\phi'\simeq\frac{V_{\mathrm{int}}'}{\hbar\omega}\propto\frac{\sqrt{I}}{\hbar\omega}\mu'\ . \quad (37)$$

Although ϕ' increases with the intensity, its values are vanishingly small throughout the entire zone of the fragmentation.

(ii) $|V_{\mathrm{int}}/\hbar\omega|\gg 1$: This regime corresponds to intensities which are prohibitively high. The state preparation problem and the extremely strong resonance overlapping are some of the severe complications that it addresses. In this regime, more than one photon is exchanged, and its study is out of the scope of the present paper. Nevertheless, within the single block description, it is important to determine the behavior of the nonadiabatic couplings. Equations (35) and (36) give

$$\phi'\to\frac{\hbar\omega}{4}\frac{V_{\mathrm{int}}'}{V_{\mathrm{int}}^2}\quad\text{as } V_{\mathrm{int}}\to\infty\ , \quad (38)$$

or, by making use of Eq. (4),

$$\phi'\to\frac{\hbar\omega}{4}\frac{1}{\mu\sqrt{I}}\frac{d}{dR}\ln V_{\mathrm{int}}\quad\text{as } V_{\mathrm{int}}\to\infty\ . \quad (39)$$

This behavior assures vanishing nonadiabatic couplings at the limit of either very high intensities or large interparticle distances [44]. As is seen from Eq. (38), this behavior holds whatever the form of the divergence of the potential coupling, since V_{int}^2 diverges faster than V_{int}'.

In the adiabatic frame both radiative and kinetic couplings vanish asymptotically. No pseudoflux is expected to be endowed in the closed-channel component U_+, and the entire width must be carried by the open-channel component U_- only. This is illustrated in Figs. 1 and 2, where both diabatic and adiabatic channel functions are shown for two different intensities. For sufficiently large R, Eq. (34) reduces to the following expression:

TABLE I. Widths and shifts (in cm^{-1} units) with respect to the corresponding zero coupling energy (78 701.56 cm^{-1}) of the $v=0$ resonance, for different intensities (in W/cm^2 units), and for $\lambda=100$ nm referring to crossing at the equilibrium position. Widths and/or shifts are calculated with the Fermi golden rule (first row) and with energy quantization including one Floquet block (second row). They are also extracted from an asymptotic analysis of the open-channel function: The Siegert analysis is from Eq. (18); the diabatic flux analysis is from Eqs. (27) and (28); the adiabatic flux analysis is from Eqs. (40) and (41). Comparison is made with the converged calculation of Ref. [23], involving many Floquet blocks. The errors indicate the stability of the widths along the last 2000 points on the real part of the grid.

$v=0$	Property	$I=3.5\times10^{10}$	$I=3.5\times10^{12}$	$I=1.4\times10^{13}$
Fermi golden rule	width	3.4222	342.22	1368.88
Energy quantization. One block	width	3.4222	377.05	1787.94
	shift	2.49	276.01	558.05
Siegert analysis: Eq. (18)	width	3.47±0.05	368±7	1565±85
Diabatic: Eq. (27)	width	3.37±0.03	372±3	1770±10
Eq. (28)	shift	7.68±1.69	754±167	2557±648
Adiabatic: Eq. (40)	width	3.4222±0.0000	377.05±0.00	1787.94±0.00
Eq. (41)	shift	2.49±0.00	276.01±0.00	558.05±0.00
Converged calculation (Ref. [23])	width	3.4295	380.48	1782.70
	shift	2.18	217.31	447.74

TABLE II. Widths and shifts (in cm^{-1} units) with respect to the corresponding zero coupling energy (95 487.76 cm^{-1}) of the $v=10$ resonance, for same laser parameters as in Table I.

$v=10$	Property	$I=3.5\times10^{10}$	$I=3.5\times10^{12}$	$I=1.4\times10^{13}$
Fermi golden rule	width	0.2239	22.39	89.56
Energy quantization. One block	width	0.2239	26.83	176.07
	shift	0.292	234.346	966.951
Adiabatic: Eq. (40)	width	0.2239±0.0000	26.83±0.00	176.07±0.00
Eq. (41)	shift	0.292±0.000	234.346±0.000	966.951±0.000

$$\frac{\Gamma}{2}=\mathrm{Im}\left[\frac{U'_-(R)}{U_-(R)}\right], \tag{40}$$

where only a single channel is involved. The corresponding expression for the resonance position reads

$$E_r=V_-(R)-\mathrm{Re}\left[\frac{U'_-(R)}{U_-(R)}\right]. \tag{41}$$

These expressions offer the possibility to check the accuracy within which the diabatic channel functions are computed and, therefore, the efficiency of complex rotation to localize resonances for divergent potential couplings. They also offer the means to measure the degree of the asymptotic decoupling of the adiabatic channels and, consequently, the quality of the adiabatic representation to describe laboratory observations for all the examined intensities. In the special case of asymptotically constant persistent couplings [21], the nonadiabatic terms are zero, due to the fact that $\phi'=\phi''=0$. The adiabatic potentials converge to constant thresholds $I_\pm$, and the open-channel component of the wave function, U_-, acquires a modified Siegert form:

$$U_-(R)\rightarrow\mathcal{A}\exp(i\mathcal{K}R), \tag{42}$$

where $\mathcal{K}=\sqrt{E-I_-}$ is the wave number of the adiabatic open channel, and $\mathcal{A}$ the corresponding amplitude. Equations (18) and (23), respectively, are modified into

$$\frac{\Gamma}{2}=|\mathcal{K}||\tilde{\mathcal{A}}|^2 \tag{43}$$

and

$$\frac{\Gamma}{2}=\mathcal{K}_0|\tilde{\mathcal{A}}|^2, \tag{44}$$

where $\tilde{\mathcal{A}}$ denotes the normalized amplitude of the open adiabatic channel and $\mathcal{K}_0$ the real part of the wave number $\mathcal{K}$, respectively.

III. RESULTS

Calculations are done for three laser intensities corresponding to different field regimes and with a wavelength $\lambda=100$ nm, which is close to the maximum of the single-photon absorption line shape of the vibrationless state. Two laser induced resonances are studied, representing a low- and a high-lying vibrational level, i.e., $(v,J)=(0,1)$ and (10,1), by propagating the Fox-Goodwin ratio matrices along a partially real grid. Both inward and outward Fox-Goodwin matrices are initialized by zero for both channel components of the resonance wave function. Various grid dimensions are tried, all leading to at least 3–4 accurate decimal digits. As a typical grid we

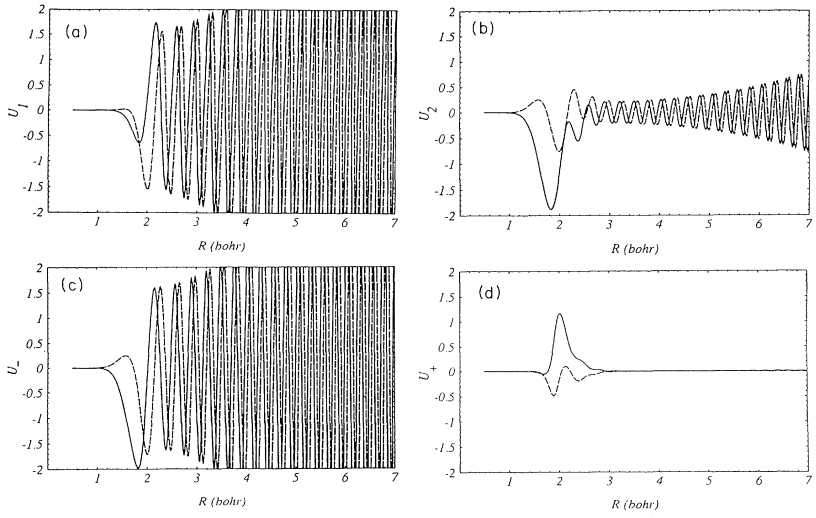

FIG. 2. Same as for Fig. 1, but for $I=1.4\times10^{13}$ W/cm^2. The closed-channel component in the diabatic frame asymptotically diverges, thus endowing a nonphysical flux. Its asymptotic contribution becomes vanishingly small in the adiabatic frame.

refer to the one consisting of 8000 points and a step size of 0.0025 bohr corresponding to a range of 20 bohr within which the fragmentation is studied. The integration path is rotated into the complex plane beyond the position R_0 in the far asymptotic region. Various scaling parameters ($R_0=7-15$ bohr, and $\theta=0.2-0.5$ rad) are tried, all leading to stable plateaus within at least three decimal digits of accuracy. The matching of the Fox-Goodwin matrices is held at the equilibrium position of the ground-state potential, $R_e=2$ bohr. For the wavelength under consideration, the dissociating state crosses the ground-state potential very close to this equilibrium position and no barrier is formed to obstruct the single-photon absorption. For an extended range of field strengths covering all the examined intensities, the flux almost entirely follows the single-photon pathway. For $v=0$ the description of the process turns out to be absolutely sufficient within a single Floquet block. This is shown in Table I, where energies and widths of the $v=0$ resonance are presented as calculated within the two-channel approach; comparison is made with results from converged multiblock calculations [23]. By inspecting Table I, the following conclusions are drawn.

(i) For the low intensity regime ($I=3.5\times10^{10}$ W/cm^2) the width of the photodissociating resonance vary linearly with the intensity, and the Fermi golden rule is applicable. In addition, the open-channel component of the wave function behaves to a very good approximation like a Siegert wave in the far outer zone, and Eq. (18) [or (23)] reproduces the width obtained from energy quantization.

(ii) As the intensity increases ($I=3.5\times10^{12}$ W/cm^2), nonlinear effects appear and the Fermi golden rule is no longer valid. Other terms in the Born expansion of the transition operator begin to contribute; however, the process still involves a net amount of one absorbed photon. For this intensity regime, Siegert analysis is partly valid, leading to a width which is not well stabilized. The indicated errors give an estimate of the instabilities throughout the last 2000 points along the real part of the integration path. Flux analysis carried out in the single-channel diabatic frame provides a width which also differs from that of single block energy quantization. The inadequacy of the single-channel diabatic analysis to extract the shift of the resonance becomes even more pronounced.

(iii) For strong intensities ($I=1.4\times10^{13}$ W/cm^2), the process is highly nonlinear, while the Siegert analysis fails

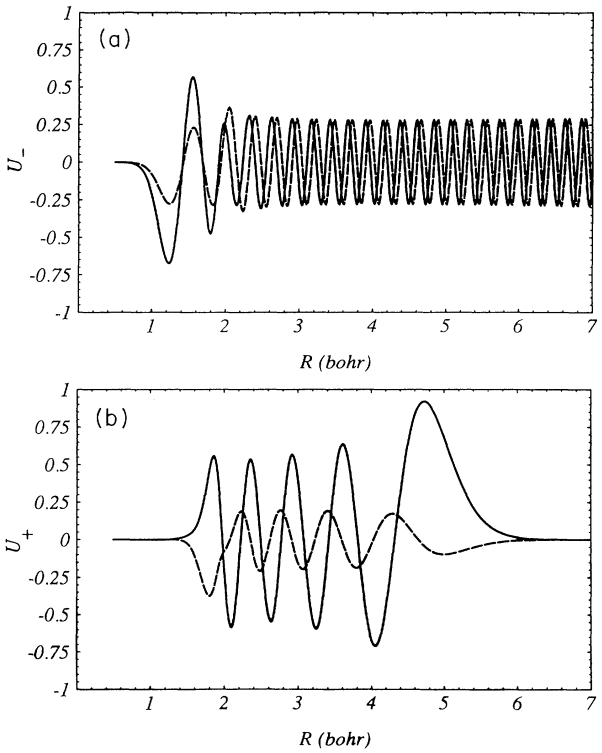

FIG. 3. Open (a) and closed (b) adiabatic channel functions of the $v=10$ resonance for $I=1.4\times10^{13}$ W/cm^2. Being confined in the upper adiabatic potential, the closed-channel function has a nodal structure similar to a $v_+=8$ *adiabatic* level.

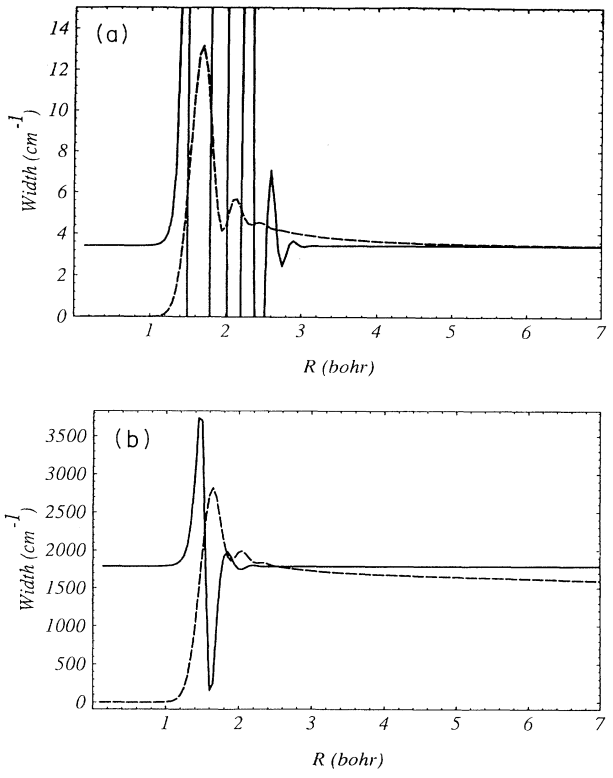

FIG. 4. Width (in cm^{-1} units) as a function of increasing interparticle distance (in bohr). (a) $I=3.5\times10^{10}$ W/cm^2. (b) $I=1.4\times10^{13}$ W/cm^2. Solid lines: through a single-channel flux analysis in the adiabatic frame [Eq. (40)]. The abrupt changes in the vicinity of the crossing position are due to the important contribution of nonadiabatic couplings. These couplings settle down asymptotically, thus producing well stabilized plateaus. Dashed lines: through a Siegert asymptotic analysis [Eq. (18)]. For low intensity (a), this analysis converges to the width from the flux; for high intensity (b), it does not converge.

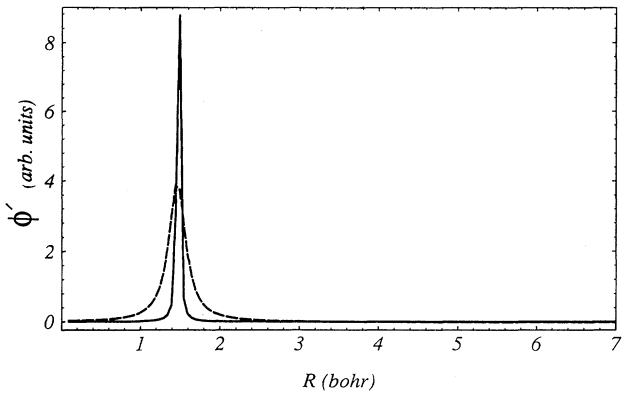

FIG. 5. Nonadiabatic couplings ϕ' (in arbitrary units) as a function of the interparticle distance (in bohr units). Solid line: $I=3.5\times10^{10}$ W/cm^2. Dashed line: $I=1.4\times10^{13}$ W/cm^2. As the intensity increases, the nonadiabatic couplings spread around the crossing position; however, they remain vanishingly small in the asymptotic region.

in reproducing the resonance width. As for the single diabatic channel expressions of Eqs. (27) and (28), where no Siegert form of the open channel is assumed, they also fail to reproduce the resonance properties.

On the other hand, for all the examined intensity regimes, Eqs. (40) and (41) are able to reproduce the width and shift of the $v=0$ resonance to an excellent accuracy (five to six figures). The high quality of the method to correctly quantize laser-induced resonances, and, through an asymptotic analysis of the open adiabatic channel function, to reproduce accurately their widths and shifts, is preserved no matter how much of the persistent couplings their wave functions experience. This is numerically demonstrated in Table II for a very high-lying resonance $v=10$, whose wave function, being spatially diffused, is much more exposed to the radiative coupling. Figures 1 and 2 refer to the $v=0$ resonance for the two extreme intensities, respectively. Figures 1(a) and 1(b) illustrate the open- and closed-channel components of the wave function in the diabatic representation. Figures 1(c) and 1(d) illustrate the corresponding components in the adiabatic representation. As long as the intensity remains low, the functions in the two frames are not characterized by important differences, and the resonance properties could be equally extracted from both frames (Fig. 1). On the contrary, as the intensity increases (Fig. 2) the closed diabatic channel function presents asymptotically an important oscillatory and diverging behavior comparable to that of the open channel. This behavior is associated with a physically unacceptable flux which carries part of the resonance width and vanishes once the adiabatic frame is invoked. A similar behavior is observed for higher-lying resonances. In Fig. 3 the open [Fig. 3(a)] and closed [Fig. 3(b)] adiabatic channel functions are presented for the resonance of quantum number $v=10$ and for the highest laser intensity ($I=1.4\times10^{13}$ W/cm^2). It should be noticed that the closed-channel component of the wave function contains eight nodes instead of ten. Although in the preparation stage the resonance stems from the $v=10$ level, its physically relevant closed-channel component has a nodal structure similar to the $v_+=8$ vibrational level of the upper adiabatic curve which is formed. The energy of this resonance (dressed by the photon) turns out to be $E_r=96\,454.71$ cm^{-1}, very close to the energy of the vibrational level $v_+=8$ of the upper adiabatic potential, i.e., 96 590.96 cm^{-1}.

The inadequacy of the Siegert analysis is illustrated on Fig. 4, where the $v=0$ resonance width from Eq. (18) is shown as a function of interfragment distance, and compared with the width from the flux analysis of the open adiabatic channel of Eq. (40) for the two extreme intensities of Table I [Figs. 4(a) and 4(b)]. For the highest intensity [Fig. 4(b)] the Siegert analysis fails completely to reproduce the width of the resonance. In Fig. 5, the behavior of the nonadiabatic couplings is illustrated as a function of increasing interparticle distance for the two extreme intensities of Table I. Apart from a region of small extent around the crossing position $R_e=2$ bohr, the nonadiabatic couplings turn out to be vanishingly small throughout the entire domain of R, thus allowing for the single open-channel adiabatic analysis of Eqs. (40) and (41).

Being asymptotically decoupled, the adiabatic channel functions are the physically relevant ones in the far asymptotic region. The Born-Oppenheimer approximation becomes exact at that limit. The width is carried only by the open-channel components of the resonance wave function. This feature is preserved even in cases where more than one open channel is involved and, therefore, opens the door to the quantitative determination of total and partial photodissociation rates for high laser intensities. This is the case of the following study (paper II), where more than one Floquet block pertains to the physics of the process, corresponding to eventual absorptions and/or emissions of more than one photon [24].

ACKNOWLEDGMENTS

Fruitful discussions with Professor T. T. Nguyen-Dang (Université Laval, Québec, Canada) are gratefully acknowledged. This work has been funded by the EEC-Science Plan program (Contract No.-SC1-CT91-0641).

*Also at UFR de Physique Fondamentale et Appliquée, Université Pierre et Marie Curie, Paris, France.

[1] C. Cornaggia, D. Normand, J. Morellec, G. Mainfray, and C. Manus, Phys. Rev. A **34**, 207 (1986).
[2] A. M. Lau and C. K. Rhodes, Phys. Rev. A **16**, 2392 (1978).
[3] J. M. Yuan and T. F. George, J. Chem. Phys. **68**, 3040 (1978).
[4] A. D. Bandrauk and M. L. Sink, J. Chem. Phys. **74**, 1100 (1981).
[5] S. I. Chu, J. Chem. Phys. A **75**, 2215 (1981).
[6] M. H. Mittleman, *Introduction on the Theory of Laser*

Atom Interactions (Plenum, New York, 1982).
[7] T. T. Nguyen-Dang and A. D. Bandrauk, J. Chem. Phys. **79**, 3256 (1983); **80**, 4926 (1984); **83**, 2840 (1985); **85**, 7224 (1986); T. T. Nguyen-Dang, in *Atomic and Molecular Processes with Short Intense Laser Pulses,* edited by A. D. Bandrauk (Plenum, New York, 1988), pp. 323.
[8] X. He, O. Atabek, and A. Giusti-Suzor, Phys. Rev. A **38**, 5586 (1988).
[9] R. W. Heather, Comput. Phys. Commun. **63**, 446 (1991).
[10] R. W. Heather and F. H. Mies, Phys. Rev. A **44**, 7560 (1991).
[11] D. Kosloff and R. Kosloff, J. Comput. Phys. **52**, 35 (1983); R. Kosloff, J. Phys. Chem. **92**, 2087 (1988).
[12] S. I. Chu, Chem. Phys. Lett. **54**, 367 (1978).
[13] W. J. Meath, R. A. Thuraisingham, and M. A. Kmetic, in *Lasers, Molecules, and Methods,* Advances in Chemical Physics Vol. 73, edited by J. O. Hirschfelder, R. E. Wyatt, and R. D. Coalson (Wiley, New York, 1989), p. 307.
[14] T. T. Nguyen-Dang and S. Manoli, Phys. Rev. A **44**, 5841 (1991).
[15] A. Giusti-Suzor, X. He, O. Atabek, and F. H. Mies, Phys. Rev. Lett. **64**, 515 (1990).
[16] F. H. Mies and A. Giusti-Suzor, Phys. Rev. A **44**, 7547 (1991).
[17] A. D. Bandrauk, E. Constant, and J. M. Gauthier, J. Phys. (France) II, **1**, 1033 (1991).
[18] O. Atabek and R. Lefebvre, Int. J. Quantum Chem. **19**, 901 (1981).
[19] Y. B. Band, K. F. Freed, and D. J. Kouri, Chem. Phys. Lett. **79**, 233 (1981); Y. B. Band and K. F. Freed, *ibid.* **79**, 238 (1981); S. Lee and K. F. Freed, J. Chem. Phys. **87**, 5772 (1987).
[20] S. C. Givertz and G. G. Balint-Kurti, J. Chem. Soc., Faraday Trans. 2 **82**, 1231 (1986).
[21] M. Chrysos and R. Lefebvre, J. Phys. B **26**, 2627 (1993).
[22] A. F. J. Siegert, Phys. Rev. **56**, 750 (1939).
[23] X. He, O. Atabek, and A. Giusti-Suzor, Phys. Rev. A **42**, 1585 (1990).
[24] M. Chrysos, O. Atabek, and R. Lefebvre, following paper, Phys. Rev. A **48**, 3855 (1993).
[25] H. Nakamura, J. Chem. Phys. **87**, 4031 (1987); M. S. Child, *Semiclassical Mechanics and Molecular Applications* (Oxford University Press, New York, 1991).
[26] W. P. Reinhardt, Ann. Rev. Phys. Chem. **33**, 223 (1982).
[27] M. L. Goldberger and K. M. Watson, *Collision Theory* (Wiley, New York, 1964), Chap. 8.
[28] C. A. Nicolaides and D. R. Beck, Phys. Lett. A **65**, 11 (1978).
[29] B. Simon, Phys. Lett. A **71**, 211 (1979).
[30] O. Atabek and R. Lefebvre, Chem. Phys. **52**, 199 (1980).
[31] F. V. Bunkin and I. I. Tugov, Phys. Rev. A **8**, 601 (1973).
[32] O. Atabek and R. Lefebvre, Chem. Phys. **55**, 395 (1981); R. Lefebvre, J. Chem. Phys. **92**, 2869 (1990).
[33] R. Lefebvre, Phys. Rev. A **46**, 6071 (1992).
[34] B. Gyarmati and T. Vertse, Nucl. Phys. A **160**, 523 (1971).
[35] D. K. Watson, Phys. Rev. A **34**, 1016 (1986).
[36] U. Fano, Phys. Rev. **124**, 1866 (1961).
[37] N. Hokkyo, Progr. Theor. Phys. **33**, 1116 (1965).
[38] J. Humblet and L. Rosenfeld, Nucl. Phys. **26**, 529 (1961).
[39] G. Jolicard and G. D. Billing, J. Chem. Phys. **97**, 997 (1992).
[40] R. S. Friedman, M. L. Du, and A. Dalgarno, J. Chem. Phys. **93**, 2375 (1990).
[41] M. H. Alexander, J. Chem. Phys. **95**, 8931 (1991).
[42] N. Moiseyev and U. Peskin, Phys. Rev. A **42**, 255 (1990).
[43] This can also be viewed as a direct consequence of a single-channel complex-energy Schrödinger equation, $HU=EU$, for a potential V assumed to be real, and for eigenenergy $E=E_r-i\Gamma/2$ which has already been provided. Thus $E=-(U''/U)+V$, from where the relations $\Gamma/2=\mathrm{Im}(U''/U)$ and $E_r=V-\mathrm{Re}(U''/U)$ are directly obtained.
[44] T. T. Nguyen-Dang (private communication).